Thermoprogrammed Desorption

A Laboratory Experiment

M. Dolores Merchán and Francisco Salvador[1]
Departamento de Química Física, Facultad de Química, Universidad de Salamanca, 37008 Salamanca, España

Processes that take place on solid surfaces form the basis of many phenomena of chemical or physicochemical interest, such as adsorption, catalysis, corrosion, and adhesion. They are of paramount importance in industry.

The characterization of the surface and the porous structure of solids are important aspects to be taken into account before conducting experiments involving reactions on the surface of a solid. It is necessary to have information about various parameters—such as surface geometry, particle size distribution, pore structure, specific surface area, composition of the adsorbed layers, the nature of and the the interaction energy between the adsorbate and the surface—when investigating surface reactions and processes that occur or begin to occur on the surface of a solid.

In recent years the number of methods for surface analysis and their potential application and sophistication have advanced considerably. Previously, *this Journal* has offered a highly detailed description of the modern methods currently available (*1–3*). In textbooks on physical chemistry, reference is made only to the classic methods (pore size, surface area, monolayer, etc.). Only in the more recent books, such as that of Atkins (*4*), is reference made to methods such as spectrophotometry and thermodesorption.

The implementation of laboratory practicals addressing this topic is usually encumbered either by the difficulties involved in using gases or the need for very costly and delicate equipment. Despite this, for some time *this Journal* has published procedures for simple practicals, such as the recording of isotherms, both in gas phase and in solution (*5–8*), the determination of specific surface areas (*5*, *9*, *10*), and even certain more complex experiments involving adsorption kinetics (*11*).

We propose a simple experiment on thermoprogrammed desorption (TPD) that any student of physical chemistry should have sufficient knowledge to understand and apply. The experimental complexity has been simplified enormously: The experiment is carried out in the condensed phase, and a slightly modified conventional HPLC system is used. TPD is a technique usually carried out in the gaseous phase, and only recently has it been carried out in solution (*12*).

Theoretical Foundations

In TPD the species adsorbed onto a solid surface is removed by the thermal excitation caused by programmed heating of the sample. The desorbed molecules are removed continuously by a vacuum or a carrier gas (in our case a carrier liquid) and are monitored by a detector, usually a mass spectrometer. Graphic plotting of the desorption rate against temperature affords the TPD spectrum (thermogram). TPD provides information about the surface, yielding the number and nature of the active sites as well as the interaction energy between the adsorbate and the surface.

[1] To whom all correspondence should be addressed.

First-Order Kinetic Process

For a better understanding, we shall consider the simplest case in which desorption is a first-order kinetic process, such that the desorption rate will be proportional to surface coverage θ.

$$v_d = -\frac{d\theta}{dt} = \beta\frac{d\theta}{dT} = Ae^{-(E_d/RT)}\theta \tag{1}$$

which takes into account the Arrhenius equation and linear heating. A is the preexponential factor; E_d is the activation energy; and β is the heating rate.

As may be seen, during desorption the rate increases exponentially with the increase in temperature but decreases as surface coverage progressively decreases. The occurrence of these tandem opposite effects means that the shape of the thermogram will be a curve with a maximum. The position of this maximum allows one to determine the value of E_d (*13*).

The temperature T_M, where the rate reaches its maximum value, can readily be obtained by imposing the condition of the maximum.

$$\frac{d\left(-\frac{d\theta}{dT}\right)}{dT} = 0 \tag{2}$$

giving the equation

$$\frac{A}{\beta}e^{-(E_d/RT)} = \frac{E_d}{RT_M^2} \tag{3}$$

in which one observes the dependence of the position of the maximum on the heating rate. This equation can thus be converted to

$$\ln\frac{T_M^2}{\beta} = \frac{E_d}{R}\frac{1}{T_M} + \ln\frac{E_d}{RA} \tag{4}$$

which gives a straight line when ln (T_M^2/β) is plotted against $1/T_M$.

The slope and the ordinate contain the values of E_d and A. Thus, study of the variation in the position of the maximum as a function of the heating rate allows one to calculate these two kinetic parameters.

Second-Order Desorption

A similar procedure can be developed for second-order desorption. In this case, the thermogram obtained is symmetric with respect to T_M. By contrast, when desorption is first-order the thermogram is asymmetric with a less pronounced slope in the ascending part of the peak than in the descending segment (*13*). However, these shapes of the thermograms may become deformed due to the readsorp-

tion phenomena (inverse reaction) or because E_d is often not constant but rather a function of coverage—when there are interactions among the molecules adsorbed.

A model in which readsorption is considered leads to a slightly more complex rate equation.

$$-\frac{d\theta}{dT} = \frac{1}{\beta}\frac{k_d\theta}{1+\frac{N_0}{F}k_a(1-\theta)} \quad (5)$$

where k_a is the rate constant of the adsorption process.

This expression shows the influence of flow rate F and sample size N_0. This expression would coincide with eq 1 when the second term of the denominator is much less than 1, that is, when $F >> N_0k_a$. This situation is achieved working with small samples and large flow rates. In some cases there may be other types of adsorption sites with different activation energies such that each of them will give a different peak in the desorption thermogram. All these complications, as well as others, often hinder correct interpretation of the thermogram. The theory of TPD is dealt with in depth in the work of Redhead (*13*), Ehrlich (*14*), Cvetanovic et al. (*15*), and Malet (*16*).

From the experimental point of view, the desorption rate is determined by following the concentrations of the desorbed species in the carrier liquid because it is not possible to measure surface coverage directly. However, it is easy to establish the following relationship between the desorption rate and concentration by a simple mass balance.

$$-\frac{d\theta}{dt} = C\frac{F}{N_0} \quad (6)$$

where C is the concentration of the desorbed species in the carrier liquid, and F is the flow rate.

Thus, the experimental thermogram represents the concentration of the carrier fluid as a function of temperature. From this, it is also easy to see that the area of the thermogram is related to the amount of substance desorbed.

Experimental

Flow System

Usually, desorption can only be achieved at such high temperatures that any solvent will be in the gaseous phase. Accordingly, for the process to occur in the condensed phase the only option is to carry out the experiment at high pressures. Although this poses an experimental difficulty, it can be solved with relative ease. To this end, the device shown in Figure 1 was constructed. It consists of a flow system situated between the pump and the detector of an HPLC apparatus.

The carrier liquid (A), generally water, is forced through the preheater (C), consisting of a tube of stainless steel, 2 m in length, 1/16-in. o.d. × 0.040-in. i.d. (Alltech Chromatography, catalog no. 3003), which is connected to the desorption chamber (D). The chamber consists of a small HPLC vacuum column, 50 mm long, 1/4-in. o.d. × 4.6-mm i.d. (Alltech Chromatography, catalog no. 9448) with filters at either end. The sample to be desorbed is placed in the vacuum column with an inert material, glass beads of 1-mm diameter (Sigma, catalog no. G 9393). The chamber (D) and preheater (C) are immersed in a thermostatic bath with silicon oil (E), which allows work at above 100 °C. This bath is connected to a homemade (*17*) or commercial thermoprogramming device (F) capable of achieving different linear heating rates.

Connected to the desorption chamber (D) is a cooler (H) built from a glass-lined metal tubing measuring 2 m long, 1/16-in. o.d. × 0.3-mm i.d. (SGE Chromatography Products, catalog no. 082710). The cooler unit is immersed in a 10-L water bath (J) and is designed to cool the desorbed species dissolved in the carrier liquid to about 25 °C before it arrives at the detector (L).

The high pressures of the system are achieved with a filter (I) and capillary tube (K) of 1.5-m length that connect the cooler to the detector of the chromatograph. (In the present study, the detector was a UV–vis spectrophotometer, which substantially increased the loss of charge of the carrier liquid.) The filter (I), which is very small, with a filtering disk of 0.5 μm is of the type used in HPLC to protect the column (Alltech Chromatography, catalog no. 05-0149). The capillary tube (K) is a highly inert plastic (PEEK, polyether ether ketone) resistant to high pressures, 1/16-in. o.d × 0.007-in. i.d. (Alltech Chromatography, catalog no. 35712).

The above characteristics of the filter and the capillary tube mean that for a carrier liquid flow of 3.5 $cm^3\ min^{-1}$ the pressure in the circuit will be higher than 50 atm, sufficient to maintain the condensed phase at high temperatures. All joints are conical to support high pressures.

Materials and Methods

As an example, the desorption of a dye crystal violet (CV^+) from silica gel was chosen because such desorption displays a maximum at relatively low temperatures (close to 100 °C). Before use, the silica gel (for chromatography, 35–70 mesh) was heated at 120 °C in an oven for 24 h.

The samples to be desorbed were previously prepared by the following method. Silica gel (2.0 g) was added to 0.5 L of a solution of CV^+ of 1.0 absorbance measured at 590 nm. Gentle stirring for several hours yields almost 90% adsorption of the dye. The silica gel is removed from the solution and washed several times with a small amount of distilled water. The silica gel is then dried in an oven at 40 °C for 2 h and stored in a desiccator.

Samples of 0.040 g are placed inside the desorption chamber with the inert material (glass beads). Then, with the selected heating rate in the programmer, the chromatograph pump is brought into operation, thus inducing the carrier liquid to circulate. The flow rate is 4.5 $cm^3\ min^{-1}$, which is sufficiently high to minimize the readsorption phenomenon. The desorbed sample is moni-

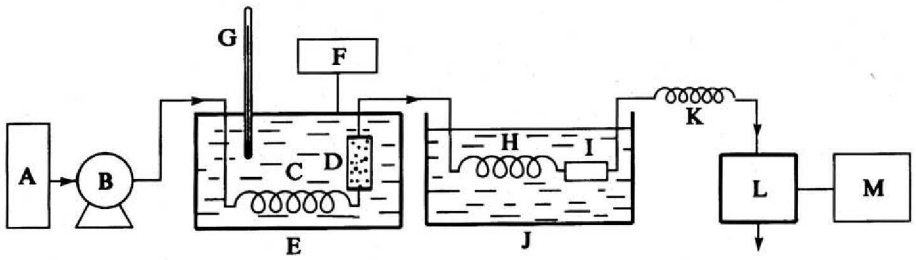

Figure 1. Schematic diagram of the thermoprogrammed desorption apparatus using the pump and the detector of a conventional HPLC apparatus; reservoir of carrier fluid (A); HPLC pump (B); preheater (C); column (D); constant temperature bath (E); temperature programmer (F); thermometer (G); refrigerant (H); protective filter (I); constant temperature bath (J); capillary tubing (K); HPLC detector (L); recorder (M).

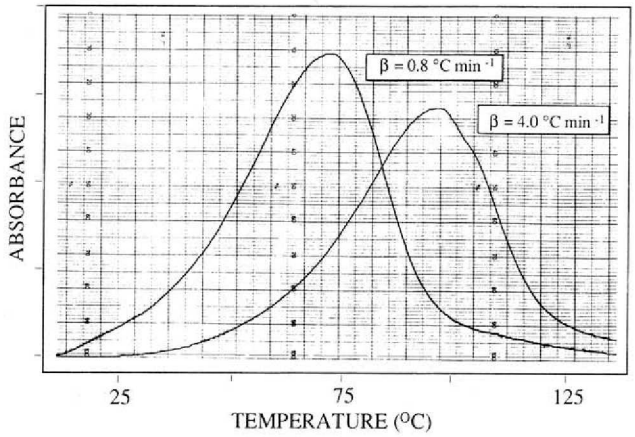

Figure 2. Thermograms of desorption of crystal violet from silica gel at two heating rates. The desorption rate is measured in units of absorbance of the carrier fluid at 590 nm and 4.5 cm^3 min^{-1}.

Table 1. Influence of Heating Rate on the Temperature of the Maximum

β (°C min^{-1})	T_M (°C)
0.441	61
0.795	70
1.099	73
1.531	78
2.186	84
3.284	92
3.973	96

gram. The heating rate is determined experimentally from the plot of the temperature of the bath versus time. The temperature of the maximum is read directly from the thermogram once plotted.

Results and Conclusions

Figure 2 shows two thermograms in the 15–125 °C range obtained with different heating rates. In both graphs, a single maximum is observed. This maximum is displaced towards higher temperatures on increasing the heating rate. Table 1 shows the position of the maximum for seven different heating rates. Fitting these data to eq 4 allows one to calculate the activation energy E_d. Figure 3 shows the plot of ln (T_M^2/β) against $1/T_M$, from whose slope one obtains a value for the activation energy of 59 kJ mol^{-1}.

The shape of the thermograms suggests a first-order process because the initial stretch of the thermogram displays a less pronounced slope than the descending part. However, in the desorption of CV^+ from silica gel the position of the maximum is influenced by the initial saturation of the sample and, to a lesser extent, by the flow rate of the carrier liquid, especially at low flow rates. All this seems to demonstrate the existence of readsorption phenomena (which are favored at low flow rates) and of the dependence of the activation energy on the fraction of surface covered. Accordingly, the value for E_d is valid within the context of the experimental conditions under which it was obtained. The value of 59 kJ mol^{-1} is consistent with the energies of the interactions due to hydrogen bonding, which are common in processes of adsorption onto silica gel.

The results obtained by students at our laboratory are around 5% of this value. The main source of error in applying the method is assigning the temperature of the maximum. Although results depend on the student conducting the experiment, this temperature may vary by several degrees. This, and the type of plot in which the experimental data undergo a strong mathematical transformation, lead to acceptable results for a laboratory experiment.

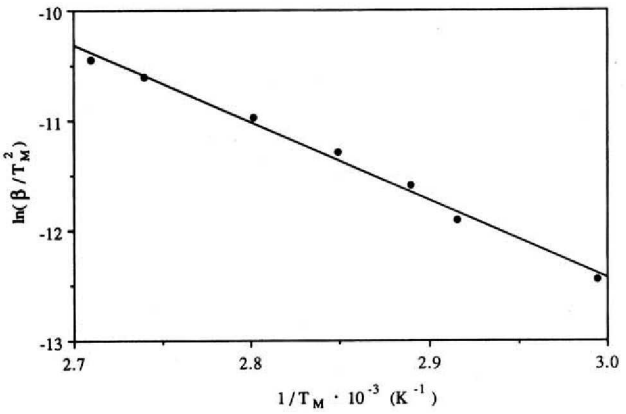

Figure 3. Calculation of the activation energy of desorption. Plot of ln (T_M^2/β) against $1/T_M$.

Table 2. Influence of Flow Rate on the Thermoprogrammed Desorption of CV^+ from Silica Gel

F (cm^3 min^{-1})	T_M (°C)
2.0	93
3.0	88
4.0	85
4.5	84
5.0	84

β = 2.19 °C min^{-1}; $\theta_0 = 2.17 \times 10^{-6}$ mol g^{-1}; mass of adsorbent, w = 0.040 g.

A more rigorous treatment of the basis of a model that considers readsorption and the dependence of the desorption energy on the degree of saturation could be carried out, although this lies outside the scope of this kind of practical. However, this practical experiment can be completed by carrying out experiments in which flow rate, sample size, initial surface coverage, etc., are varied; these would point to the existence of such phenomena.

Of the above parameters, flow rate exerts the greatest influence on the position of the thermogram. Table 2 shows the results. The thermogram is displaced towards lower temperatures when flow rate is increased and becomes stable around 84 °C.

Literature Cited

1. Hercules, D. M.; Hercules, S. H. *J. Chem. Educ.* **1984**, *61*(5), 402–409.
2. Hercules, D. M.; Hercules, S. H. *J. Chem. Educ.* **1984**, *61*(6), 483–489.
3. Hercules, D. M.; Hercules, S. H. *J. Chem. Educ.* **1984**, *61*(7), 592–599.
4. Atkins, P. W. *Physical Chemistry*, 4th ed.; Oxford University: Oxford, 1990; p 873.
5. Dunicz, B. L. *J. Chem. Educ.* **1961**, *38*(7), 357–358.
6. Hanson, J. C.; Stafford, F. E. *J. Chem. Educ.* **1965**, *42*(2), 88–91.
7. Blazer, D. *J. Chem. Educ.* **1974**, *51*(12), 827–829.
8. Duff, D. G.; Ross, S. M. C.; Vanghan, D. H. *J. Chem. Educ.* **1988**, *65*(9), 815–816.
9. Brina, R.; De Battisti, A. *J. Chem. Educ.* **1987**, *64*(2), 175–176.
10. Potgieter, J. H. *J. Chem. Educ.* **1991**, *68*(4), 349–350.
11. Casado, J.; Salvador, F.; Rincón, S. *J. Chem. Educ.* **1985**, *62*(9), 800–802.
12. Salvador, F.; Merchán, M. D. *Langmuir* **1992**, *8*, 1226–1229.
13. Redhead, P. A. *Vacuum* **1962**, *12*, 203–211.
14. Ehrlich, G. *Advn. in Catal.* **1963**, *14*, 255–427.
15. Cvetanovic, R. J.; Amenomiya, Y. *Catal. Rev.* **1972**, *6*(1), 21–48.
16. Malet, P. *Stud. Surf. Sci. Catal., Spectrosc. Charact. Catal. pt(B)* **1990**, *42*, 333–383.
17. Salvador, F; Gonzalez, J. L.; Tel, L. M. *J. Chem. Educ.* **1985**, *62*, 613.